Characterization of Membrane Protein Non-native States. 1. Extent of Unfolding and Aggregation of Rhodopsin in the Presence of Chemical Denaturants[†]

Arpana Dutta,[‡] Kalyan C. Tirupula,[‡] Ulrike Alexiev,[§] and Judith Klein-Seetharaman*,[‡]

[‡]*Department of Structural Biology, University of Pittsburgh School of Medicine, Pittsburgh, Pennsylvania 15260, and*
[§]*Institut für Experimentalphysik, Freie Universität Berlin, Arnimallee 14, D-14195 Berlin, Germany*

ABSTRACT: Little is known about the general folding mechanisms of helical membrane proteins. Unfolded, i.e., non-native states, in particular, have not yet been characterized in detail. Here, we establish conditions under which denatured states of the mammalian membrane protein rhodopsin, a prototypic G protein coupled receptor with primary function in vision, can be studied. We investigated the effects of the chemical denaturants sodium dodecyl sulfate (SDS), urea, guanidine hydrochloride (GuHCl), and trifluoroacetic acid (TFA) on rhodopsin's secondary structure and propensity for aggregation. Ellipticity at 222 nm decreases in the presence of maximum concentrations of denaturants in the order TFA > GuHCl > urea > SDS + urea > SDS. Interpretation of these changes in ellipticity in terms of helix loss is challenged because the addition of some denaturants leads to aggregation. Through a combination of SDS−PAGE, dependence of ellipticity on protein concentration, and 1D ^{1}H NMR we show that aggregates form in the presence of GuHCl, TFA, and urea but not in any concentration of SDS, added over a range of 0.05%−30%. Mixed denaturant conditions consisting of 3% SDS and 8 M urea, added in this order, also did not result in aggregation. We conclude that SDS is able to prevent the exposure of large hydrophobic regions present in membrane proteins which otherwise leads to aggregation. Thus, 30% SDS and 3% SDS + 8 M urea are the denaturing conditions of choice to study maximally unfolded rhodopsin without aggregation.

Membrane proteins are essential for all living systems and include important protein families such as receptors, transporters, ion channels, pumps, and proteins with structural roles or enzymatic activity. In humans, membrane proteins constitute one-third of all the proteins (*1*). Failure of a membrane protein to fold into its native three-dimensional structure can lead to disruption of regulated cell functions and cause diseases (*2*). There are several pathological conditions such as cystic fibrosis, Charcot−Marie−Tooth disease, hearing loss, and retinitis pigmentosa (RP), in which misfolding of membrane proteins has been implicated as contributing to disease (*2*). Through an understanding of the folding mechanisms of membrane proteins it may be possible to identify avenues for the treatment of such diseases.

In the field of soluble proteins, characterization of unfolded states has been crucial in understanding mechanisms of folding and indeed has shed light also on misfolding diseases (*3, 4*). An important conclusion is that even under strongly denaturing conditions some interresidue interactions, either native-like or non-native and especially those among hydrophobic residues, are present in the unfolded state (*5*). Such interactions constitute residual structure in denatured states and are assumed to form during the early stages of folding of a protein, playing a crucial role for folding by acting as a folding nucleus (*5*). Non-native interactions of unstructured peptide fragments for example are believed to play a major role in amyloid formation in Alzheimer's

disease (*6*). In principle, any protein sequence has an intrinsic propensity to aggregate, and even form amyloid fibrils (*4*), but point mutations can enhance this propensity as has been shown for example for transthyretin and lysozyme (*7, 8*). While these mutations do not alter the structure of the folded state, they change structure and stability of unfolded states and result in accumulation of folding intermediates (*7, 9*). Based on the characterization of these folding intermediates, therapeutic strategies have been proposed such as blocking fibrillar growth by β-sheet breaker peptides (*10*) and stabilizing native structure of these proteins by small molecules (*11−13*).

In contrast to soluble proteins, little is known about unfolded states of membrane proteins, and there have been few efforts to date toward understanding the molecular mechanisms of membrane protein folding in general. It has been proposed in the two-stage hypothesis that the initial stages of folding of helical membrane proteins involve primarily formation of the helices (*14, 15*), while the long-range interaction hypothesis emphasizes contact formation involving residues in loops connecting the helices (*16, 17*). Experimental testing of such mechanistic hypotheses is challenging mainly due to the difficulties in perturbing these protein systems, in which high stability arises from the hydrophobic environment of the membrane. In order to accommodate the hydrophobic nature of membrane proteins, they need to be reconstituted in a detergent or lipid environment to maintain their functionality, which also renders them resistant toward denaturation. In vitro folding/unfolding studies of membrane proteins require optimization of denaturing conditions that would lead to a significant degree of unfolding. Another challenge faced by denaturation experiments is formation of aggregates due to exposure of large hydrophobic regions of membrane proteins.

The first work on the folding of membrane proteins was carried out with bacteriorhodopsin (bR) which was successfully refolded into phospholipids via transfer into sodium dodecyl sulfate (SDS)[1] micelles after denaturation by trifluoroacetic acid (TFA) (18). This has established bR as a model system for studying the folding of helical membrane proteins (19). Kinetic studies of refolding of bR from an SDS-denatured state into lipid/detergent micelles have enabled detection of folding intermediates in its folding pathway (20–24). Efforts on elucidating the folding pathways of other membrane proteins are underway. Refolding has been possible for the bacterial membrane proteins KcsA, from a trifluoroethanol- (TFE-) denatured state (25), DAGK and DsbB from SDS-denatured states (26, 27), and EmrE from a SDS + urea denatured state (28) and for the LHCII complex from higher plants from a SDS-denatured state (29, 30). In all of these cases, however, refolding was accomplished only from a partially unfolded, near native state. Recently, studies with opsin in phospholipid bicelles revealed a significant decrease of 50% in its helical content in the presence of urea, but it could not be refolded from such a largely unfolded state (31). Therefore, refolding of membrane proteins except bR is typically feasible only from a minimally denatured state which is structurally very similar to the native state but becomes difficult when large portions of the structure are unfolded.

While reversibility of unfolding is crucial for kinetic and thermodynamic studies of folding, it is not a requirement for biophysical characterization of denatured states. Here, the requirements are long-term stability of the denatured state of interest without aggregation. Further, the extent of unfolding is important. To catch a glimpse of the earliest stages in folding, ideally the protein is denatured to the maximum possible extent. In this paper, we therefore describe our efforts on chemical denaturation of rhodopsin in dodecyl maltoside (DM) detergent micelles by addition of SDS, TFA, urea, and guanidine hydrochloride (GuHCl). We find that 4 M TFA disrupts secondary structure of rhodopsin to the greatest extent, followed by 8 M GuHCl, 10 M urea, 3% SDS + 8 M urea, and 30% SDS in decreasing order in their extent of denaturation. However, aggregation of rhodopsin in the presence of urea, GuHCl, and TFA precludes further investigation of these denatured states. In contrast, 30% SDS and 3% SDS + 8 M urea are found to be the most suitable denaturants to study unfolding of rhodopsin due to their largest extent of denaturation without formation of aggregates. As per our knowledge, this is the first time that unfolding and detection of aggregates of a membrane protein have been described in a systematic manner.

MATERIALS AND METHODS

Materials. SDS (electrophoresis grade) was purchased from Bio-Rad (Hercules, CA) and dodecyl maltoside (DM) from Anatrace (Maumee, OH). Rhodopsin was isolated from bovine retinae and purified in 2 mM sodium phosphate buffer, pH 6, in the presence of 0.05% DM as described previously (32).

Methods. Circular Dichroism Spectroscopy. CD spectra were recorded using a Jasco J-810 spectrometer (Jasco Inc., Easton, MD). Rhodopsin (1.5 μM) in 2 mM sodium phosphate buffer, pH 6, and 0.05% DM in the presence of different concentrations of denaturants was placed in a 1 mm quartz cell.

All spectra were recorded at 25 °C with a bandwidth of 1 nm, scan speed of 100 nm/min, and a response time of 1 s. Each spectrum was reported as an average of 10 spectra. Spectra recorded in the absence of denaturant and in the presence of up to 3% SDS, 3 M urea, and 3 M GuHCl were subtracted from the corresponding buffer reference spectra containing 70 μM nonamer peptide used during rhodopsin purification. For spectra of solutions containing more than 3% SDS, 3 M urea, 3 M GuHCl, and all concentrations of TFA, sodium phosphate buffer containing 0.05% DM and appropriate denaturant concentration without nonamer were subtracted. This was because very small volumes of highly concentrated rhodopsin were added to the working solution to achieve a final concentration of 1.5 μM resulting in dilution of the nonamer to levels undetectable by CD spectroscopy. Note that while the subtraction of nonamer peptide affects ellipticity at 208 nm, the change in ellipticity at 222 nm is small and amounts to a maximum decrease in absolute ellipticity of about 5% (for 70 μM peptide, Figure 1). Most solutions contained less concentrations of the peptide. The effect of denaturants over time was monitored by recording CD scans every 0.5 h for a period of 14 h. All CD spectra were analyzed using CDPro software (33). The helicity was estimated by using CDPro by taking the basis set (no. 10) containing both soluble proteins and membrane proteins (33).

A python script was developed as a user interface for running CDPro. The script takes as input the CD spectra in millidegrees (θ), path length of cuvette (l in cm), concentration of protein (c in molar units), and number of amino acids in protein (n) and calculates molar circular dichroism or delta epsilon ($\Delta\varepsilon = \theta/(10lcn \times 3298)$) which is used as input by the CDPro software. The script by default executes all the three secondary structure determining algorithms CONTIN/LL (33, 34), SELCON3 (35), and CDSSTR (36) available within CDPro. There is also an option provided in the script for the user either to choose the basis set suggested by CDPro or to use all available basis sets for data processing. The script generates two plain text (comma separated value format) files: (1) wavelength versus calculated mean residue ellipticity ([θ] = $\Delta\varepsilon \times 3298$) and (2) reformatted output of CDPro that can be opened by any spread sheet or plotting programs for further analysis. This script is available at http://jks-lab.structbio.pitt.edu/CD.

SDS−Polyacrylamide Gel Electrophoresis (*SDS−PAGE*). SDS−PAGE analysis of rhodopsin at different denaturant concentrations was performed at 200 V for 30 min on a 10% SDS−PAGE. SDS concentration was 0.1% in the buffers used to make the stacking and resolving parts of the gel. The electrophoresis buffer also contained 0.1% SDS. Nonreducing Laemmli dye (Bio-Rad, Hercules, CA), consisting of 62.5 mM Tris, pH 6.8, 2% SDS, 25% glycerol, and 0.01% bromophenol blue, was used in 1:1 ratio to load native rhodopsin on the gel. The effect of additional SDS in the nonreducing Laemmli dye on denatured samples was negated by the use of native gel loading dye. The latter in 2× concentration contained 25% glycerol and 0.01% bromophenol blue and was used to load denaturant (SDS and/or urea) containing samples of rhodopsin on the gel. Silver staining was done using the SilverSNAP stain kit (Thermo Scientific, Waltham, MA).

One-Dimensional [1]*H NMR*. All NMR measurements were performed at 25 °C using a Bruker 800 MHz spectrometer. Samples containing 50 μM rhodopsin in 20 mM sodium phosphate buffer (pH 6.0), 1% DM, and 10% D_2O in the presence and absence of SDS were used to record the NMR spectra.
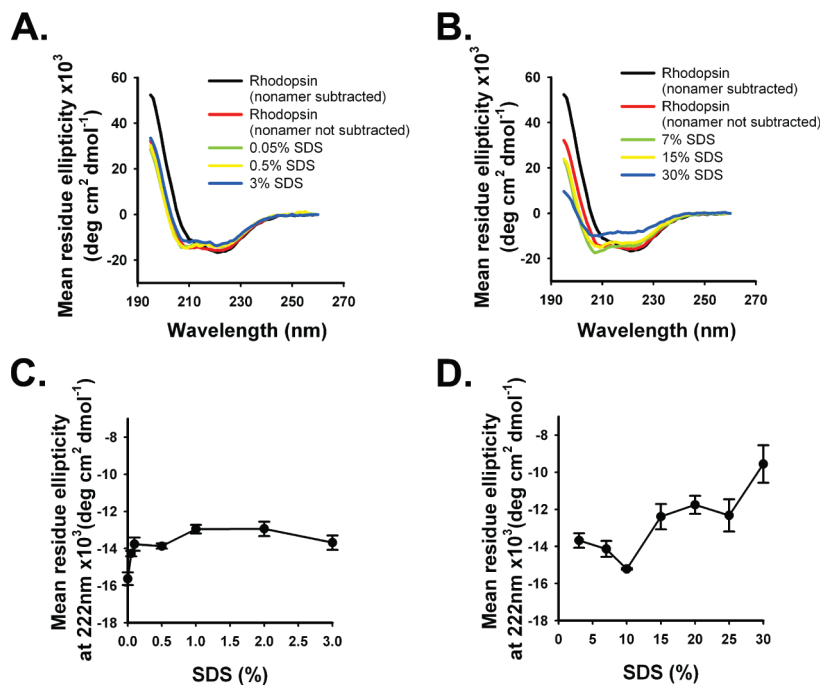
FIGURE 1: SDS-induced denaturation of rhodopsin monitored by CD spectroscopy. CD spectra of 1.5 μM rhodopsin (black line) alone and in the presence of (A) 0.05%−3% and (B) 7%−30% SDS concentrations. Total mean residue ellipticity at 222 nm of rhodopsin in the presence of (C) 0.05%−3% SDS and that in the presence of (D) 7%−30% SDS. All CD spectra in (A) are subtracted from the corresponding buffer spectrum containing 70 μM nonapeptide, and those in (B) are subtracted from buffer alone because of reasons stated in the Materials and Methods section. Spectra of rhodopsin (nonamer not subtracted) correspond to a concentration of 1.5 μM obtained after dilution from a very high concentrated protein sample thus resulting in amounts of nonamer undetectable by CD.

One-dimensional ^{1}H NMR spectra were recorded using a selective excitation scheme with sculpting that utilizes a double pulse field gradient spin echo sequence (DPFGSE) (*37, 38*). A total of 2048 scans were averaged to obtain the final spectrum at each condition. A line broadening of 1 Hz was used to process final spectra.

Cysteine Accessibility Measurements. 4,4′-Dithiodipyridine (4-PDS) reacts with free sulfhydryl groups in cysteines to produce stoichiometric amounts of 4-thiopyridone that absorbs at 323 nm (*39*), and the reaction was used to quantify cysteine accessibility of rhodopsin essentially as described (*40*). The number of cysteines reacting with 4-PDS per molecule of rhodopsin was estimated by taking the ratio of the absorbance at 323 nm and that at 500 nm and multiplying it with the ratio of the molar extinction coefficient of rhodopsin (40600 M^{-1} cm^{-1}) and that of 4-thiopyridone (19000 M^{-1} cm^{-1}). Rhodopsin (1.5 μM) in 2 mM sodium phosphate buffer, pH 6, and 0.05% DM was reacted with 37.5 μM 4-PDS in the sample cuvette at 25 °C. The same amount of 4-PDS was added to the reference cuvette. The reaction was followed spectrophotometrically by recording the changes in absorbance spectra over time. At the end of the experiment, when the 323 nm peak reached saturation, all spectra were subtracted from the original rhodopsin spectrum in the absence of 4-PDS.

Steady-State Fluorescence Spectroscopy. Fluorescence measurements were carried out using a Varian Cary Eclipse fluorescence spectrophotometer (Varian Inc., Palo Alto, CA). Emission scans of 1.5 μM rhodopsin in 2 mM sodium phosphate buffer, pH 6, and 0.05% DM titrated with GuHCl were recorded in the wavelength range 310−500 nm with an excitation wavelength of 295 nm. Excitation and emission slit widths were kept at 5 and 10 nm, respectively. Medium photomultiplier tube voltage was applied, and measurements were taken at a scan rate of

600 nm/min. For time course measurements, fluorescence emission at 330 nm was recorded every 30 min. All experiments were carried out at 25 °C.

RESULTS

Secondary structure of rhodopsin in the presence of different chemical denaturants (SDS, urea, GuHCl, TFA, and combinations thereof) was assessed by circular dichroism. While solvent background precluded measurements at very low wavelengths for some of the conditions, at the very minimum the range including ellipticity at 222 nm, most important for assessment of helical structure content, was obtained for all conditions. For each denaturant, we also established whether or not aggregation occurs. Here, the methods varied depending on the denaturant because some approaches are not applicable to some denaturants. The results are summarized in Table 1 and are described below in order of denaturant. Thus, for each denaturant, there is a description of the effects on secondary structure, followed by the effects on rhodopsin aggregation.

SDS as a Denaturant of Rhodopsin: Disruption of Secondary Structure. To measure the loss of secondary structure in the presence of increasing amounts of SDS, rhodopsin was titrated with varying concentrations of SDS, and the circular dichroism (CD) spectrum was recorded at each concentration. CD spectra of rhodopsin (1.5 μM) alone and in the presence of low concentrations of SDS up to 3% are shown in Figure 1A, and those in the presence of high SDS concentrations up to 30% are shown in Figure 1B. The corresponding plots of mean residue ellipticity (MRE) at 222 nm are shown in panels C and D of Figure 1, respectively. The magnitude of MRE at 222 nm decreases abruptly at a concentration of 0.05% SDS and then remains essentially constant with increasing SDS concentrations

Table 1: Summary of Biophysical Techniques Used to Detect Aggregates

| denaturants	concn range	techniques used for detection of aggregates					
		CD	SDS–PAGE	NMR	Trp fluorescence	Cys accessibility	by eye
SDS	0%–30%	no dependence of MRE on [rhodopsin]	no oligomeric bands	no broad peaks representing aggregates	shown in accompanying paper (DOI 10.1021/bi00339x) for analyses of tertiary structure changes	shown in accompanying paper (DOI 10.1021/bi00339x) for analyses of tertiary structure changes	no precipitates detected
urea	0–10 M	not done since clear from SDS–PAGE and visual detection	oligomeric bands	cannot be done since aggregates are formed as seen by eye	not done since sufficient evidence from SDS–PAGE and visual detection	not done since sufficient evidence from SDS–PAGE and visual detection	precipitates detected
SDS + urea	3% SDS + 8 M urea	not done since clear evidence from SDS–PAGE	no oligomeric bands, aggregation seen only when urea is added before adding SDS	not done since clear evidence from SDS–PAGE	not done since clear evidence from SDS–PAGE	not done since clear evidence from SDS–PAGE	no precipitates detected
GuHCl	0–8 M	dependence of MRE on [rhodopsin]	GuHCl buffer alone precipitates on addition of Laemmli dye	cannot be done since aggregates are formed as seen by eye	shows a decrease at 8 M after an increase at 3 M	shows a decrease at 8 M after an increase in 3 M	precipitates detected
TFA	100 mM and 4 M	not done since precipitates were detected by eye and large background signals from buffer alone	not done since precipitates were detected by eye	cannot be done since aggregates are formed as seen by eye	not done since precipitates were detected by eye	not done since precipitates were detected by eye	precipitates detected
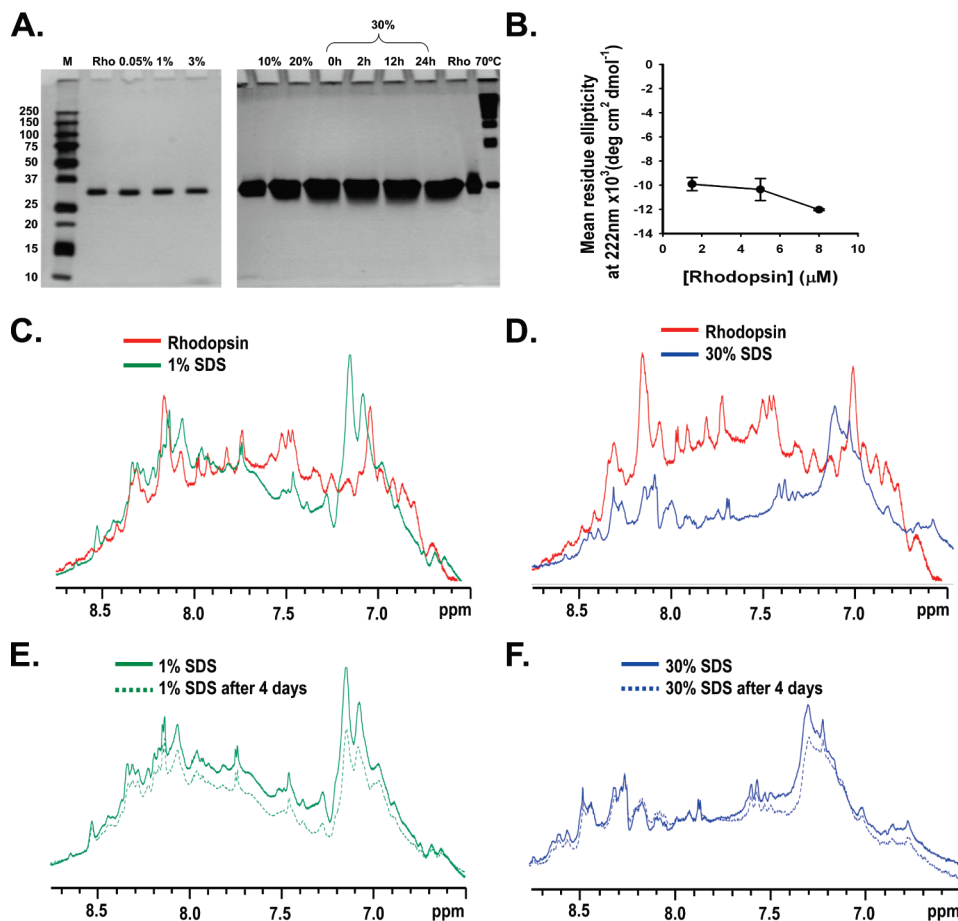
FIGURE 2: (A) Silver-stained 10% SDS−polyacrylamide gel of rhodopsin in the presence of SDS. First gel: lane 1, marker; lane 2, native rhodopsin; lanes 3, 4, and 5, rhodopsin in 0.05% SDS, 1% SDS, and 3% SDS, respectively. Second gel: lanes 2 and 3, rhodopsin in 10% and 20% SDS, respectively; lanes 4, 5, 6, and 7, rhodopsin in 30% SDS at time t = 0, 2, 12, and 24 h, respectively; lane 8, rhodopsin; lane 9, rhodopsin denatured at 70 °C. (B) Plot showing changes in MRE at 222 nm on rhodopsin concentration during SDS denaturation. 1D proton spectra showing overlay of (C) rhodopsin and rhodopsin in 1% SDS, (D) rhodopsin and rhodopsin in 30% SDS, (E) rhodopsin in 1% SDS, and (F) 30% SDS after 4 days of incubation with that after immediate SDS addition.

until 3% (Figure 1C). The decrease in the magnitude of MRE at 222 nm at 3% SDS is $12 \pm 2\%$, which corresponds to an estimated ~19% decrease in helicity calculated using CDPro software (*33*). However, already at 2% SDS, a slight increase in the magnitude of MRE begins which reaches a maximum at 10% SDS (Figure 1D). Subsequently, a large decrease in the magnitude of MRE values at 222 nm is observed as the SDS concentration is raised beyond 10% up to 30% as shown in Figure 1D. The change in MRE at 222 nm is $39 \pm 6\%$ at 30% SDS, indicating loss of substantial amounts of native helical regions. The corresponding decrease in helicity, as approximated using CDPro software, is ~45%.

In order to ensure that the values recorded at each SDS concentration correspond to the maximal denaturation by SDS at that concentration, rhodopsin was incubated with 0.05%, 1.5%, 3%, and 30% SDS overnight at 25 °C. Loss of secondary structure was monitored by CD spectroscopy every 30 min during the incubation period, but no time-dependent further denaturation was observed (data not shown).

The changes in CD spectra (shown in Figure 1A) with increasingly higher concentrations of SDS added to rhodopsin are summarized in Figure 1C by mean ellipticity at 222 nm as a function of SDS concentration. SDS concentrations up to 3% show two distinct stages, an initial decrease in helicity followed by no change up to 3% SDS. The CD results at higher SDS concentrations

are shown in panels B and D of Figure 1. A third stage over the range of SDS concentrations 3%−10% SDS can be clearly seen in the CD spectrum in Figure 1B and summarized in Figure 1D: a distinct increase in the magnitude of MRE at 222 nm is observed in this range. In a fourth stage (15%−30% SDS), a sudden decrease in helicity to a large extent at concentrations beyond 15% SDS.

SDS as a Denaturant of Rhodopsin: Detection of Aggregates. The above studies strongly suggest that high concentrations of SDS are very well suited to denature rhodopsin. In order to be able to characterize the molecular nature of such states, it is imperative that no aggregation occurs in the presence of SDS. We therefore tested for aggregation using multiple complementary methods, including SDS−PAGE, dependence of molar ellipticity on rhodopsin concentration, and ^{1}H NMR spectroscopy.

First, we looked for aggregates on SDS−PAGE (Figure 2A,B). Native loading dye (see Methods) was used so that no additional amount of SDS is introduced from the sample loading buffer and the result is not an effect of its addition. This is especially critical for the samples containing low concentrations of SDS such as 0.05%, 1%, and 3%. The possibility that SDS present in the gel and running buffer (0.1% SDS in each) would dissolve the aggregates we are trying to detect is highly unlikely. This is because we are detecting for aggregates caused by SDS denaturation;
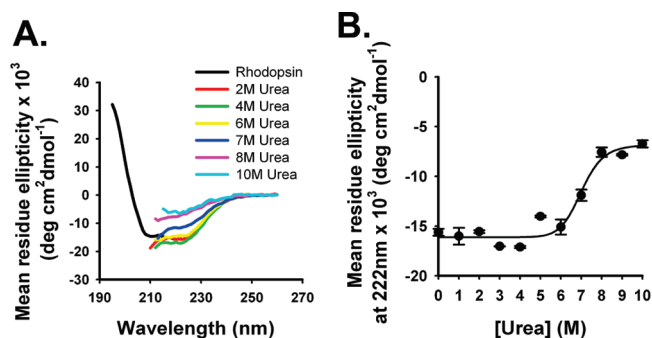
A.

B.

FIGURE 3: Urea-induced denaturation of rhodopsin monitored by CD spectroscopy. (A) CD spectra of 1.5 μM rhodopsin (black line) alone and in the presence of urea concentration from 2 to 10 M. (B) Mean residue ellipticity at 222 nm of rhodopsin in the presence of 1−10 M urea.

i.e., the samples already contain SDS, and if aggregates are present, they would be dissolved in the sample even before loading on the gel. Further, the amount of SDS that we have used to denature rhodopsin is significantly higher than what is present in the gel and running buffer, thus ruling out the contribution of SDS in the gel system, other than that in the samples, to influence our results.

Figure 2A shows a silver-stained polyacrylamide gel with native rhodopsin in lane 2 (Rho). Native rhodopsin runs as a band between 37 and 25 kDa on SDS−PAGE, and the same gel shows rhodopsin denatured with 0.05%, 1%, and 3% SDS in lanes 3, 4, and 5, respectively. These samples were loaded using native loading dye (see Methods). As can be seen from these gels, a single band at the same position as native rhodopsin is observed for rhodopsin in the presence of different concentrations of SDS tested, indicating no changes in electrophoretic mobility of SDS-denatured states compared to that of native rhodopsin. The adjacent gel shows rhodopsin denatured with 10%, 20%, and 30% SDS in lanes 2, 3, and 4, respectively, as compared to native rhodopsin (Rho) in lane 8. These samples were also loaded with native dye (see Methods). To check the stability over time, rhodopsin was incubated with 30% SDS for 2 h (lane 5), 12 h (lane 6), and 24 h (lane 7). A single band in the same position as that of native rhodopsin was also observed during longer incubation of rhodopsin in the presence of 30% SDS, suggesting that SDS-denatured rhodopsin is stable over long periods of time and no aggregation is observed even after 24 h of incubation. Rhodopsin denatured by heating at 70 °C in lane 9 was run as a positive control for aggregation. In contrast to the lack of aggregation in the presence of SDS, the positive aggregation control shows higher molecular weight oligomeric bands.

Since none of the SDS concentrations used showed evidence for aggregation and we are interested in the most denaturing conditions, we further corroborated lack of aggregation at 30% SDS by testing if the CD spectra showed any sign of dependence on rhodopsin concentration. CD spectra of rhodopsin denatured with 30% SDS were recorded at increasing protein concentrations of 1.5, 5, and 8 μM. There was little if no dependence of MRE at 222 nm on protein concentration (Figure 2B). This further supports the absence of aggregation at the maximum SDS concentration used (30%), even at higher rhodopsin concentrations.

Finally, we further corroborated the lack of aggregation in SDS using ^{1}H NMR spectroscopy. Proton peaks arising from a natively folded protein are dispersed across the range of approximately −1 to 10 ppm. Peaks corresponding to amide protons are

found mainly in the region from 6.5 to 10 ppm. For a disordered or completely unfolded protein, all amide protons in similar chemical environment cluster together around 8 ppm impairing resolution. In case of aggregated protein, loss of peak dispersion accompanied by an increase in line widths of proton peaks is expected. We therefore further checked for the lack of aggregation in SDS-denatured states by recording one-dimensional proton NMR spectra of rhodopsin in the absence and presence of SDS. To avoid interference from detergent signals, these spectra were obtained by selective excitation of the protein backbone region by using a sculpting scheme as described (*37, 38*). Overlay of the proton spectra, showing the backbone region of rhodopsin alone and in the presence of 1% SDS, is displayed in Figure 2C. The peaks in native rhodopsin correspond mostly to the flexible regions of rhodopsin that become sharper on adding 1% SDS. The peaks between 7.2 and 6.8 ppm in the native state coalesce to form a sharper peak in 1% SDS-denatured state. Figure 2D shows the overlay between native rhodopsin and that in the presence of 30% SDS. Here again, the peaks become sharper in the presence of 30% SDS compared to the native state. Peaks between 7.2 and 6.8 ppm appear to merge, giving rise to a sharper peak in the presence of 30% SDS. However, the overall peak intensity suffers a decrease in the presence of 30% SDS when compared to that of native rhodopsin. This may be due to slow tumbling of the large cylindrical SDS micelles that are formed at 30% SDS. These 1D spectra show absence of aggregation since an aggregated protein sample would have given rise to broad peaks. No significant changes were seen in these spectra even after 4 days, indicating absence of any time-dependent aggregation (Figure 2E,F).

Urea as a Denaturant of Rhodopsin: Disruption of Secondary Structure. Next, we measured the effect of urea on rhodopsin by CD spectroscopy. Rhodopsin (1.5 μM) was titrated with different concentrations of urea, and the CD spectrum was recorded at each concentration, as shown in Figure 3A. The change in MRE at 222 nm as a function of urea concentration is shown in Figure 3B. A two-stage unfolding behavior was observed. Essentially, no change in secondary structure of rhodopsin occurs up to 6 M urea. This is followed by a steep decrease by 57% in the magnitude of MRE at 222 nm in the range between 6 and 10 M urea. This is greater than the extent of denaturation by 30% SDS. The midpoint of the unfolding transition is at 7 M urea. No time-dependent change in ellipticity was observed when rhodopsin was incubated with 10 M urea for 12 h (data not shown).

Urea as a Denaturant of Rhodopsin: Detection of Aggregates. Urea denaturation disrupts helical content of rhodopsin to a large extent (see above). These largely unfolded states will be suitable for further analyses only if aggregation does not occur. Thus, we checked for aggregation in the presence of urea by two methods, SDS−PAGE and dependence of MRE at 222 nm on rhodopsin concentration.

Rhodopsin treated with different concentrations of urea was run on SDS−PAGE to check for aggregation as shown in Figure 4. Native gel loading dye was used to run urea containing rhodopsin samples so that SDS present in Laemmli dye does not influence our results (see Materials and Methods). The second lane in Figure 4A corresponds to native rhodopsin. In subsequent lanes, rhodopsin immediately after addition of 4, 6, 7, and 8 M urea are shown. Oligomeric bands were seen from 7 M urea denaturation onward. This is also the urea concentration at which urea begins to significantly unfold rhodopsin (see
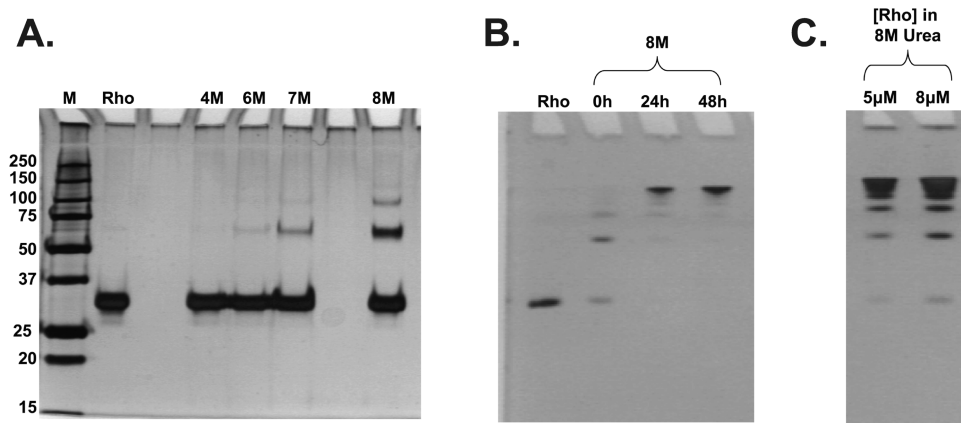
FIGURE 4: Silver-stained 10% SDS−polyacrylamide gel of rhodopsin in the presence of different concentrations of urea. (A) Lane 1, marker; lane 2, native rhodopsin; lanes 3, 4, 5, and 6, rhodopsin with 4, 6, 7, and 8 M urea, respectively, after time t = 0 of addition of urea. (B) Lane 2, native rhodopsin; lanes 3, 4, and 5, 1.5 μM rhodopsin in 8 M urea after 0, 24, and 48 h, respectively. (C) Lanes 1 and 2, 5 and 8 μM rhodopsin with 8 M urea, respectively.
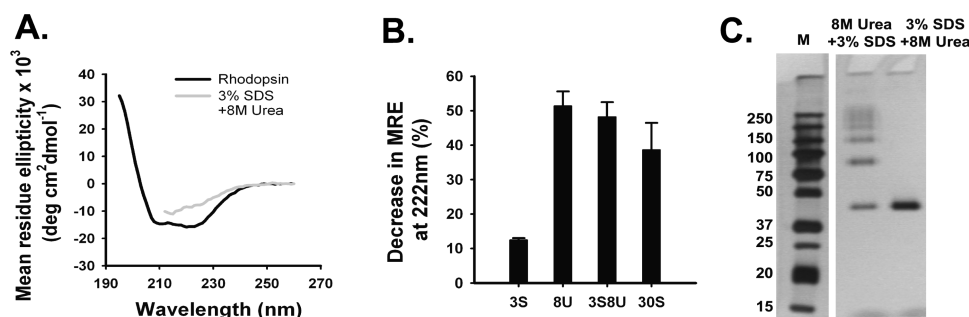

FIGURE 5: 3% SDS + 8 M urea induced denaturation of rhodopsin monitored by CD spectroscopy. (A) CD spectra of 1.5 μM rhodopsin (black line) alone and in the presence of SDS + urea (gray line). (B) Bar graph comparing percent decrease in MRE at 222 nm under different denaturing conditions of 3% SDS (3S), 8 M urea (8U), 3% SDS + 8 M urea (3S8U), and 30% SDS (30S). (C) Silver-stained 10% SDS−polyacrylamide gel of rhodopsin treated with 8 M urea + 3% SDS (8U3S) (lane 2) showing aggregation and 3% SDS + 8 M urea (3S8U) (lane 3) without any aggregates. Lane 1 shows the marker.

Figure 3). Thus, we conclude that rhodopsin begins to aggregate as soon as urea starts to unfold it. Stability of urea-denatured states was determined by incubating 1.5 μM rhodopsin with 8 M urea for 0 h (lane 2), 24 h (lane 3), and 48 h (lane 4) (Figure 4B). The time course of urea denaturation clearly shows aggregation becoming worse with time. Increase in the extent of aggregation with increase in rhodopsin concentration denatured by 8 M urea was seen by comparing lanes 1 (5 μM rhodopsin) and 2 (8 μM rhodopsin) in Figure 4C with that of rhodopsin at 1.5 μM in lane 2 in Figure 4B.

Dependence of MRE at 222 nm on rhodopsin concentration in the presence of 8 M urea was analyzed also by CD spectroscopy. As shown above, aggregation is observed on the gel from 7 M urea denaturation onward. We therefore chose a concentration of 8 M urea for this experiment. Thus, we denatured rhodopsin at increasing concentrations of 1.5, 5, and 8 μM with 8 M urea. The CD spectrum at each of the rhodopsin concentrations was recorded (data not shown). However, precipitates already were detected by eye when 8 μM rhodopsin was treated with 8 M urea, indicating aggregation of rhodopsin and thus making further analysis by CD unnecessary. Thus, appearance of aggregates precludes the use of urea as a suitable denaturant for unfolding studies of rhodopsin.

3% SDS + 8 M Urea Mixture as a Denaturant of Rhodopsin: Disruption of Secondary Structure. SDS caused a significant extent of denaturation of rhodopsin without causing
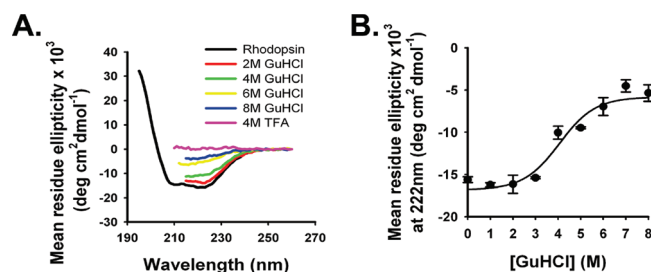

FIGURE 6: GuHCl- and TFA-induced denaturation of rhodopsin monitored by CD spectroscopy. (A) CD spectra of 1.5 μM rhodopsin (black line) alone and in the presence of GuHCl concentration from 2 to 8 M and 4 M TFA. (B) Mean residue ellipticity at 222 nm of rhodopsin in the presence of 1−8 M GuHCl.

aggregates whereas urea denatured secondary structure of rhodopsin to a greater extent than SDS but caused aggregation. We therefore tested if a mixed denaturant condition consisting of both SDS and urea could result in an extent of denaturation similar to or greater than that of urea but without aggregation. Concentrations of 3% SDS and 8 M urea were chosen because addition of more than 3% SDS and 8 M urea led to large increase in the total volume and dilution of the protein concentration. Also, 8 M urea led to a similar degree of disruption of secondary structure as 10 M urea, the latter being the maximum urea concentration that can be used. A 44% decrease in MRE at 222 nm was observed when rhodopsin (1.5 μM) was treated with 3%
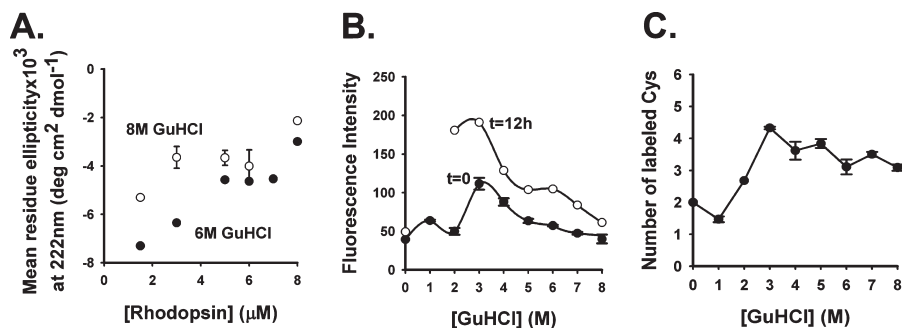
A.

B.

C.

FIGURE 7: Aggregation under GuHCl deanaturing condition. (A) Plot showing linear dependence of MRE at 222 nm on rhodopsin concentration on adding 6 M (filled circle) and 8 M (open circle) GuHCl. (B) Changes in fluorescence intensity at 330 nm in the presence of 0−8 M GuHCl immediately after its addition (filled circle) and after incubation for 12 h (open circle). (C) Number of cysteines reactive to 4-PDS in different concentrations of GuHCl ranging from 0 to 8 M.

SDS followed by addition of 8 M urea as indicated by the CD spectrum shown in Figure 5A. A similar decrease in MRE at 222 nm was also observed when rhodopsin was first treated with 8 M urea followed by addition of 3% SDS (data not shown). Comparison of the extent of denaturation by 3% SDS (3S), 8 M urea (8U), 3% SDS + 8 M urea (3S8U), and 30% SDS (30S) is shown in Figure 5B. As can be seen in this figure, addition of 8 M urea to 3% SDS-denatured rhodopsin decreases the helicity to a much greater extent than that by 3% SDS alone. Also, the mixed denaturant leads to a similar extent of denaturation as that by 8 M urea and is slightly greater than that by 30% SDS.

3% SDS + 8 M Urea Mixture as a Denaturant of Rhodopsin: Detection of Aggregates. As described in the CD experiments above, the mixture of denaturants leads to a significant decrease in the secondary structure content of rhodopsin. To determine if this condition leads to aggregation, we ran the denatured samples on SDS−PAGE as shown in Figure 5C. Samples were loaded using native dye (see Methods). Lane 2 shows the presence of aggregates when rhodopsin is treated with 8 M urea first followed by 3% SDS. This indicates irreversible aggregation by 8 M urea that cannot be rescued by addition of 3% SDS. However, no aggregates were detected on addition of 3% SDS followed by 8 M urea to rhodopsin, as shown in lane 3. Therefore, 3% SDS + 8 M urea, added in this order, is a suitable condition for studying denatured states of rhodopsin.

GuHCl and TFA as Denaturants of Rhodopsin: Disruption of Secondary Structure. Two other denaturants, GuHCl and TFA, were tested. The CD spectra of rhodopsin (1.5 μM) titrated with different concentrations of GuHCl are shown in Figure 6A. A plot of the change in MRE at 222 nm as a function of GuHCl concentration is shown in Figure 6B. Similar to the urea-induced denaturation, a two-stage behavior is seen on GuHCl unfolding. Here, the midpoint of transition was at 4 M GuHCl, as compared to the midpoint of the unfolding transition in urea of 7 M (see above). The decrease in MRE at 222 nm at 8 M GuHCl is 66%; no time-dependent decrease in helicity was observed when rhodopsin was incubated with 8 M GuHCl for 12 h (data not shown).

Finally, an organic solvent, TFA, known for its strong denaturing properties and previous denaturation power in the case of bacteriorhodopsin (*18*) was tested. TFA (4 M) was seen to disrupt rhodopsin almost completely as seen by the absence of a CD signal in the spectrum shown in Figure 6A. However, 4 M TFA buffer alone gave a strong CD signal, making the quantification of the signal unreliable. Lower concentrations of TFA

were also tested. For example, TFA at a concentration of 100 mM is the highest concentration with minimal signal background. However, this concentration led to a relatively small decrease of only ∼12% in MRE at 222 nm (data not shown).

GuHCl and TFA as Denaturants of Rhodopsin: Detection of Aggregates. GuHCl denaturation results in a large decrease in MRE at 222 nm as seen from CD spectroscopy, and TFA denaturation resulted in complete disappearance of the CD signal, indicating complete disruption of secondary structure of rhodopsin. Thus, TFA could potentially be the best denaturant if it also does not cause aggregation. Unlike for other denaturing conditions described above, SDS−PAGE analysis could not be performed for GuHCl-containing samples as precipitation was observed when Laemmli buffer was added. Furthermore, native loading dye could not be used to run GuHCl-denatured samples as they remained stuck in the wells of the gel. We therefore checked for aggregation under both GuHCl and TFA denaturation conditions by determining the dependence of MRE at 222 nm on rhodopsin concentration. For GuHCl denaturation we also measured tryptophan fluorescence and accessibility of cysteine in denatured states.

The CD spectra of rhodopsin at different concentrations of 1.5, 3, 5, 6, 7, and 8 μM each denatured with 6 M GuHCl and that of 1.5, 3, 5, 6, and 8 μM each denatured with 8 M GuHCl were recorded. Dependence of the molar ellipticity at 222 nm on protein concentration was observed at both 6 and 8 M GuHCl concentrations tested (Figure 7A). This indicates that rhodopsin oligomerizes under these conditions, and the greater decrease in MRE at 222 nm that is observed in Figure 6 may be merely an aggregation effect.

To check for aggregation in TFA-denatured samples, different concentrations of rhodopsin at 1.5, 5, and 8 μM were denatured with 4 M TFA, and a CD spectrum was recorded for each of them. A dependence of MRE at 222 nm on rhodopsin concentration was seen, but it could not be clearly determined due to high absorbance at 222 nm by buffer alone (data not shown). However, aggregates were clearly detected by eye after 3 days of preparing the samples.

Indirect evidence for aggregation in GuHCl also came from fluorescence spectroscopy. There are five tryptophan residues in rhodopsin. Their fluorescence in dark-adapted rhodopsin is quenched due to energy transfer to the retinal chromophore. The release of retinal, e.g., following light activation and decay of the activated metarhodopsin II species to free retinal and opsin, causes an increase in tryptophan fluorescence (*41*). Thus, fluorescence spectroscopy of rhodopsin is a sensitive probe for

rhodopsin structure. Furthermore, aggregation would be expected to decrease rhodopsin fluorescence by way of quenching of tryptophan fluorescence through intermolecular interactions. The changes in tryptophan fluorescence intensity at 330 nm as a function of GuHCl concentration are plotted in Figure 7B. An initial increase in tryptophan fluorescence was seen up to 3 M GuHCl. This is consistent with the disruption of retinal−protein interaction as the protein begins to unfold, similar to what would be seen by the retinal leaving the binding pocket after light activation. With further increase in GuHCl concentration up to 8 M, a decrease in fluorescence counts was observed. This is contrary to the significant unfolding of rhodopsin that occurs in the range 3−8 M GuHCl as judged by CD spectroscopy (see above). Therefore, this result supports the notion that rhodopsin aggregates under these conditions, which is expected to lead to a quenching of fluorescence. A similar pattern of change in fluorescence was also observed on longer incubation of rhodopsin with GuHCl (Figure 7B).

Finally, we also investigated aggregation indirectly through protein accessibility measurements. Analogous to fluorescence measurements, tertiary structure and aggregation of rhodopsin can be probed by cysteine accessibility. Accessibility of cysteine residues was probed using the cysteine derivatizing agent, 4,4′-dithiodipyridine (4-PDS). 4-PDS reacts with the accessible free sulfhydryl groups of cysteines, releasing stoichiometric amounts of 4-thiopyridone which has an absorption maximum at 323 nm (*39*). Of the six free cysteines in rhodopsin, only two of them can be derivatized in the dark state whereas all six of them can be derivatized upon loss of 11-*cis*-retinal on light activation (*42*). The effect on reactivity of cysteines to 4-PDS in GuHCl-denatured states was checked. An increase in cysteine accessibility to four cysteines was seen up to 3 M GuHCl (Figure 7C). Further increase in GuHCl concentration to 8 M showed a decrease in the number of cysteines reacting with 4-PDS to three (Figure 7C). This pattern is similar to the decrease seen in tryptophan fluorescence. Burial of both tryptophans and cysteines, occurring at the same concentration of GuHCl, indicates formation of aggregates. Taken together, these experiments suggest that GuHCl and TFA are not suitable denaturants for characterizing unfolded states of rhodopsin due to their aggregation properties.

DISCUSSION

Membrane proteins are notoriously difficult to unfold (*19*) due to the challenge of perturbing the surrounding stable membrane environment. In this paper we aimed at achieving a largely denatured state of rhodopsin *in vitro* in order to mimic what might be corresponding to an *in vivo* early unfolded intermediate. Computational and single molecule studies with the mammalian membrane protein rhodopsin have suggested that complex folding mechanisms may have to be considered to describe the folding of this protein (*16, 17, 43, 44*). Thus, in-depth studies of denatured states are needed to better understand these mechanisms. The characterization of unfolded states of rhodopsin, however, is still in a preliminary stage. The present paper aims to systematically compare different denaturing conditions with the aim of identifying conditions that maximally denature rhodopsin without aggregation. Because detergents such as DM do not interfere with spectroscopic techniques as compared to other membrane mimetics, we conducted all of our studies with rhodopsin reconstituted in DM. DM is a favorable detergent for rhodopsin studies because it maintains maximum rhodopsin function (*45, 46*).
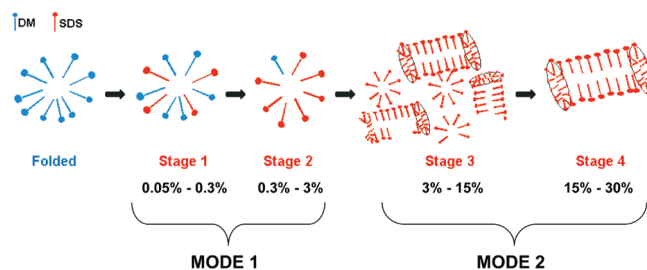

Figure 8: Models representing changes in SDS (in red) micellar structure on increasing addition of SDS to DM (in blue) micelles. DM spherical micelles form DM/SDS mixed micelles in stage 1 upon SDS addition, stage 2 represents increase in SDS spherical micelles on further adding SDS, stage 3 represents transition to cylindrical micellar formation with further increase in [SDS], sand tage 4 represents formation of SDS cylindrical micelles.

Despite the spectroscopic and functional advantages of using DM, the thermal stability of rhodopsin in DM micelles is the same as compared to that in native membranes (*47, 48*). While this is favorable for ensuring functional relevance of measurements in DM, it also makes it equally difficult to study unfolding of rhodopsin by *in vitro* denaturation experiments as if we were working with membranes. Here, we report the results of screening different denaturants to arrive at conditions that lead to maximum unfolding of rhodopsin without causing its aggregation. The former was assessed by CD spectroscopy and the latter by different techniques depending on the suitability for the specific denaturant under investigation.

The use of CD spectroscopy for determining extent of denaturation was mostly qualitative because of the known interference of aggregation. Therefore, MRE at 222 nm was mainly used to report on the degree of disruption of secondary structure instead of calculating percent helicity by deconvoluting the CD spectra. MRE at 222 nm is strongly influenced by conformation of residues in a helix, length of helix, number of helices, distribution of residues in these helices, fluctuations of a helix, and the dielectric constant of the surrounding medium (*49, 50*). These parameters have an important contribution toward helicity estimation in the case of denatured proteins. However, in the absence of suitable basis sets for denatured membrane proteins, compared to which software such as CDPro estimate the helicity (*33*), it is difficult to derive these parameters quantitatively from CD spectra. We therefore primarily relied on MRE at 222 nm values to describe secondary structure loss during denaturation in the Results section. Since it was found that basis sets in CDPro containing only soluble proteins when used for quantifying secondary structure of membrane proteins yield reasonably accurate, albeit not quantitative results when considering α-helix content alone, we did estimate the extent of decrease in helicity as a qualitative indicator of the extent of unwinding of helices. This would provide the reader with some qualitative indication about the extent of denaturation being achieved.

SDS as a Denaturant. SDS has been commonly used as a denaturant for both membrane proteins (*26, 27, 51, 52*) and soluble proteins (*53−58*). It was shown that the modes of unfolding depend on the SDS concentration range used, and indeed SDS-induced unfolding of soluble proteins correlates with changes in SDS micellar structure (*59, 60*). At low concentrations of up to 100 mM, SDS forms spherical micelles which convert into cylindrical micelles at concentrations above 6% where the

aggregation number of SDS increases from 63 to 91 (*61*). These cylindrical micelles, also referred to as "mode 2" micelles, are known to have more aggressive protein denaturation properties than the cylindrical micelles (*60*). Rapid unfolding occurs in this mode due to the large number of SDS molecules interacting with the protein and enveloping it in its large cylindrical structures. Under high SDS concentration conditions, the transition state is stabilized, and thus the energy barrier to unfolding is decreased.

Because native rhodopsin as a membrane protein is maintained in DM detergent micelles, we propose that we expect four stages in detergent properties based on these published SDS properties. These stages are visualized schematically in Figure 8. At low concentrations of SDS, we expect that the SDS displaces the DM molecules in the micelles to form SDS/DM mixed micelles. Thus, stage 1 (0.05%−0.3% SDS) represents spherical DM/SDS mixed micelles. As the SDS concentration increases, the contribution of the relatively small concentration of DM decreases, so that stage 2 (0.3%−3% SDS) is dominated by the vast excess of SDS in the spherical micelles. Stage 3 (3%−10% SDS) marks the transition from spherical to cylindrical SDS micelle shapes. Stage 4 (15%−30% SDS) is then dominated by the cylindrical micellar structures of SDS. [Note that the use of the word "stages" merely intends to reference the different ranges in SDS concentration and does not imply a temporal progression of rhodopsin structure during denaturation.]

Below, we discuss our rhodopsin denaturation by SDS in light of these stages. In the first stage of unfolding, at low [SDS] of 0.05%−0.3%, a modest decrease in the magnitude of MRE at 222 nm was seen which saturated at a value of ∼12% in stage 2 at [SDS] up to 3%, which corresponds to 100 mM. Stage 3 is a transition, when SDS is going from spherical to cylindrical "mode 2" micelles (see Figure 8) (*61*). SDS concentrations between 3% (100 mM) and 15% (500 mM) form this stage as the increase in aggregation number of SDS beyond 6% (200 mM) leads to a very large number of SDS molecules interacting with rhodopsin. As a result, we see an increase in the magnitude of MRE at 222 nm at 10% SDS to a value close to the native state indicating that SDS is inducing non-native helices, a well-known property of SDS. Stage 4 is then dominated by cylindrical micellar structures of SDS (see Figure 8) that surround largely unfolded states of rhodopsin. Here, we see a ∼40% decrease in MRE at 222 nm at 30% SDS (1 M). We estimate the extent of decrease in helicity on adding 30% SDS as a qualitative indicator of the extent of unwinding of helices and obtained a value of approximately 45%. This is consistent with "mode 2" unfolding in which SDS cylindrical micelles wrap around the membrane protein and aggressively unfold it (*59*, *60*). Formation of cylindrical micelles by SDS is also supported by 1D ^{1}H NMR experiments. A decrease in overall peak intensities of 30% SDS-denatured rhodopsin as compared to the native form can be attributed to slow tumbling of the large cylindrical micelles that are formed at such high SDS concentrations.

In order for SDS-denatured conditions to qualify for biophysical studies of denatured rhodopsin, we checked for aggregation. No aggregation of rhodopsin was detected based on multiple lines of evidence. SDS-denatured rhodopsin did not show any oligomeric bands on SDS−PAGE. By using CD spectroscopy, a dependence of ellipticity at 222 nm on protein concentration would be expected if there are aggregates forming. Such dependence was not seen when rhodopsin at different concentrations was denatured by 30% SDS, the maximum concentration of SDS used here. Further, proton peaks on the NMR spectrum of

SDS-denatured rhodopsin did not show any significant broadening compared to its native state; even after 4 days of incubation with 1% and 30% SDS, the spectrum remained almost the same. However, there was a decrease in overall signal intensity of 30% SDS denatured state compared to the native state. This may be due to formation of cylindrical micelles of SDS which tumble slowly or technical difficulties due to the high buffer concentrations or protein aggregation. Since aggregation has been ruled out by SDS−PAGE and CD spectroscopy, and no peak broadening was seen on NMR spectra of SDS-treated rhodopsin, we conclude that the decreased intensity of the proton peaks is not due to aggregation. This is consistent with the notion that aggregation of rhodopsin, being a membrane protein, is less likely in the presence of SDS because even though SDS is denaturing, it does provide a hydrophobic environment. Here, the hydrophobic amino acids that will be exposed due to unfolding still remain surrounded by the hydrophobic tails of SDS and thus are shielded from the aqueous medium preventing aggregation. These results indicate that the maximum concentration of SDS of 30% is a desirable condition for future unfolding studies of rhodopsin.

Urea as a Denaturant. Urea has been used very recently to study denaturation of opsin, a retinal-free form of rhodopsin, in phospholipid/detergent bicelles where it was shown to irreversibly unfold opsin to a significant extent (*31*). It was shown that 4 M urea could denature opsin as measured by a decrease in MRE at 222 nm by ∼50%. In our study also, a significant degree of unfolding of rhodopsin in DM micelles with urea is seen but at a much higher concentration of urea; i.e., 8 M urea could decrease MRE at 222 nm by 57%. This is mostly due to differences in the degree of intrinsic stability of opsin and rhodopsin which is also influenced by the micellar system in which they are reconstituted. It appears that the native state of opsin is less stable than that of rhodopsin. It is also possible that urea-denatured opsin is less prone to aggregation because no precipitates by eye and change in sample absorbance, reported by voltage changes in the photomultiplier tube, occurred during time course studies by CD, indicating absence of light scattering and hence aggregation (*31*). We found this method to be less reliable in detecting aggregation in our studies because they only detect very large aggregates. While we also did not detect aggregation by these methods in our studies, we did detect them based on SDS−PAGE and analysis by eye at higher rhodopsin concentrations. It is likely that aggregation is caused by exposure of large hydrophobic regions of rhodopsin due to its unfolding in urea. A way to mask these hydrophobic parts of the protein could prevent it from oligomerizing. For this reason, we tested a mixture of 8 M urea and 3% SDS as a denaturant so that SDS can be effective in screening the hydrophobic residues from water. While aggregates are detected when 3% SDS was added to 8 M urea-denatured rhodopsin, no aggregates are detected on reversing the order of addition of the denaturants. This further supports our theory that the cause of aggregation of rhodopsin in 8 M urea is exposure of hydrophobic parts, which if masked by SDS before being denatured by 8 M urea does not lead to aggregation. The extent of denaturation in 3% SDS + 8 M urea is found to be similar to that by 8 M urea and slightly greater than that by 30% SDS, thus making it a favorable denaturing condition to study unfolded states.

GuHCl and TFA as Denaturants. GuHCl denaturation leads to a decrease in MRE at 222 nm of rhodopsin by a greater extent compared to the above-mentioned denaturing conditions.

TFA, a strong denaturing condition, leads to the maximum decrease in MRE at 222 nm compared to all of the denaturants tested. It leads to a complete disappearance of CD signal indicating complete unfolding of secondary structure. However, both of these conditions also lead to formation of aggregates, thus impairing their use in further unfolding studies. For GuHCl denaturation, MRE at 222 nm depended on rhodopsin concentration indicating aggregation. TFA-induced unfolding led to precipitation after 3 days of TFA addition to rhodopsin indicating aggregation. The cause of aggregation is again likely due to the exposure of hydrophobic residues as with urea. However, SDS could not be added to mask exposed hydrophobic amino acids so that aggregation can be prevented, since precipitation occurred when SDS and GuHCl buffers were mixed together.

CONCLUSIONS

In this paper, we have screened different denaturing conditions, SDS, urea, SDS + urea, GuHCl, and TFA, for maximum unfolding without formation of aggregates. Rhodopsin denaturation is measured in terms of decrease in MRE at 222 nm. TFA denatured rhodopsin to the maximum extent (∼100%) compared to all of the denaturants tested but led to aggregation precluding its use as a good denaturant. GuHCl was the next best at denaturing rhodopsin (66% decrease in MRE at 222 nm) followed by urea (57% decrease in MRE at 222 nm), but rhodopsin aggregated under both of these conditions. Thus, urea and GuHCl, which are effective denaturants for soluble proteins, are not ideally suited for studying folding mechanisms of the membrane protein rhodopsin. SDS (30%) proved to be a suitable denaturing condition as it denatured rhodopsin significantly (40% decrease in MRE at 222 nm) without aggregating it. Also, the mixture of 3% SDS and 8 M urea is a favorable condition as it denatures rhodopsin to a similar extent as that by 30% SDS (44% decrease in MRE at 222 nm) and does not aggregate it. We conclude that SDS, either alone or in combination with urea, is a very suitable denaturant, due to the large degree of unfolding of rhodopsin in its presence and due to its ability to mask exposed hydrophobic stretches of largely unfolded membrane protein by its long hydrocarbon tails, thus preventing them from aggregation.

It is an important open question for soluble and membrane proteins alike to what extent unfolded states exist at all and in particular *in vivo*. Theoretical considerations suggest that a fully unfolded denatured state does not exist (*62*) and proteins are known to fold cotranslationally (*63, 64*). For membrane proteins, folding within the translocon has to be considered in addition. However, folding in solution and in the translocon seems to share similarities (*65*), and understanding the unfolded states is important in understanding what drives membrane protein folding. Thus, there is much to be learned from the investigation of unfolded states of membrane proteins *in vitro*. Since it is unlikely that a completely unfolded state exists *in vivo* within a membrane environment, deciphering where the regions with highest propensity for residual structure in membrane proteins are located is expected to shed light on understanding the mechanisms of membrane protein folding *in vitro* and *in vivo*.

REFERENCES

1. Takeda, S., Kadowaki, S., Haga, T., Takaesu, H., and Mitaku, S. (2002) Identification of G protein-coupled receptor genes from the human genome sequence. *FEBS Lett. 520*, 97–101.
2. Sanders, C. R., and Myers, J. K. (2004) Disease-related misassembly of membrane proteins. *Annu. Rev. Biophys. Biomol. Struct. 33*, 25–51.
3. Chiti, F., and Dobson, C. M. (2009) Amyloid formation by globular proteins under native conditions. *Nat. Chem. Biol. 5*, 15–22.
4. Dobson, C. M. (2001) The structural basis of protein folding and its links with human disease. *Philos. Trans. R. Soc. London, Ser. B 356*, 133–145.
5. Klein-Seetharaman, J., Oikawa, M., Grimshaw, S. B., Wirmer, J., Duchardt, E., Ueda, T., Imoto, T., Smith, L. J., Dobson, C. M., and Schwalbe, H. (2002) Long-range interactions within a nonnative protein. *Science 295*, 1719–1722.
6. Harper, J. D., and Lansbury, P. T., Jr. (1997) Models of amyloid seeding in Alzheimer's disease and scrapie: mechanistic truths and physiological consequences of the time-dependent solubility of amyloid proteins. *Annu. Rev. Biochem. 66*, 385–407.
7. Booth, D. R., Sunde, M., Bellotti, V., Robinson, C. V., Hutchinson, W. L., Fraser, P. E., Hawkins, P. N., Dobson, C. M., Radford, S. E., Blake, C. C., and Pepys, M. B. (1997) Instability, unfolding and aggregation of human lysozyme variants underlying amyloid fibrillogenesis. *Nature 385*, 787–793.
8. Sekijima, Y., Wiseman, R. L., Matteson, J., Hammarstrom, P., Miller, S. R., Sawkar, A. R., Balch, W. E., and Kelly, J. W. (2005) The biological and chemical basis for tissue-selective amyloid disease. *Cell 121*, 73–85.
9. Canet, D., Sunde, M., Last, A. M., Miranker, A., Spencer, A., Robinson, C. V., and Dobson, C. M. (1999) Mechanistic studies of the folding of human lysozyme and the origin of amyloidogenic behavior in its disease-related variants. *Biochemistry 38*, 6419–6427.
10. Soto, C., Sigurdsson, E. M., Morelli, L., Kumar, R. A., Castano, E. M., and Frangione, B. (1998) Beta-sheet breaker peptides inhibit fibrillogenesis in a rat brain model of amyloidosis: implications for Alzheimer's therapy. *Nat. Med. 4*, 822–826.
11. Johnson, S. M., Wiseman, R. L., Sekijima, Y., Green, N. S., Adamski-Werner, S. L., and Kelly, J. W. (2005) Native state kinetic stabilization as a strategy to ameliorate protein misfolding diseases: a focus on the transthyretin amyloidoses. *Acc. Chem. Res. 38*, 911–921.
12. Ray, S. S., Nowak, R. J., Brown, R. H., Jr., and Lansbury, P. T., Jr. (2005) Small-molecule-mediated stabilization of familial amyotrophic lateral sclerosis-linked superoxide dismutase mutants against unfolding and aggregation. *Proc. Natl. Acad. Sci. U.S.A. 102*, 3639–3644.
13. Soldi, G., Plakoutsi, G., Taddei, N., and Chiti, F. (2006) Stabilization of a native protein mediated by ligand binding inhibits amyloid formation independently of the aggregation pathway. *J. Med. Chem. 49*, 6057–6064.
14. Popot, J. L., and Engelman, D. M. (1990) Membrane protein folding and oligomerization: the two-stage model. *Biochemistry 29*, 4031–4037.
15. Engelman, D. M., Chen, Y., Chin, C. N., Curran, A. R., Dixon, A. M., Dupuy, A. D., Lee, A. S., Lehnert, U., Matthews, E. E., Reshetnyak, Y. K., Senes, A., and Popot, J. L. (2003) Membrane protein folding: beyond the two stage model. *FEBS Lett. 555*, 122–125.
16. Klein-Seetharaman, J. (2005) Dual role of interactions between membranous and soluble portions of helical membrane receptors for folding and signaling. *Trends Pharmacol. Sci. 26*, 183–189.
17. Tastan, O., Yu, E., Ganapathiraju, M., Aref, A., Rader, A. J., and Klein-Seetharaman, J. (2007) Comparison of stability predictions and simulated unfolding of rhodopsin structures. *Photochem. Photobiol. 83*, 351–363.
18. Huang, K. S., Bayley, H., Liao, M. J., London, E., and Khorana, H. G. (1981) Refolding of an integral membrane protein. Denaturation, renaturation, and reconstitution of intact bacteriorhodopsin and two proteolytic fragments. *J. Biol. Chem. 256*, 3802–3809.
19. Booth, P. J., and Curnow, P. (2006) Membrane proteins shape up: understanding in vitro folding. *Curr. Opin. Struct. Biol. 16*, 480–488.
20. Booth, P. J., Flitsch, S. L., Stern, L. J., Greenhalgh, D. A., Kim, P. S., and Khorana, H. G. (1995) Intermediates in the folding of the membrane protein bacteriorhodopsin. *Nat. Struct. Biol. 2*, 139–143.
21. Riley, M. L., Wallace, B. A., Flitsch, S. L., and Booth, P. J. (1997) Slow alpha helix formation during folding of a membrane protein. *Biochemistry 36*, 192–196.
22. Booth, P. J., and Farooq, A. (1997) Intermediates in the assembly of bacteriorhodopsin investigated by time-resolved absorption spectroscopy. *Eur. J. Biochem. 246*, 674–680.
23. Booth, P. J., Farooq, A., and Flitsch, S. L. (1996) Retinal binding during folding and assembly of the membrane protein bacteriorhodopsin. *Biochemistry 35*, 5902–5909.
24. Allen, S. J., Curran, A. R., Templer, R. H., Meijberg, W., and Booth, P. J. (2004) Folding kinetics of an alpha helical membrane protein in phospholipid bilayer vesicles. *J. Mol. Biol. 342*, 1279–1291.
25. Barrera, F. N., Renart, M. L., Molina, M. L., Poveda, J. A., Encinar, J. A., Fernandez, A. M., Neira, J. L., and Gonzalez-Ros, J. M. (2005)

Unfolding and refolding in vitro of a tetrameric, alpha-helical membrane protein: the prokaryotic potassium channel KcsA. *Biochemistry 44*, 14344–14352.

26. Lau, F. W., and Bowie, J. U. (1997) A method for assessing the stability of a membrane protein. *Biochemistry 36*, 5884–5892.

27. Otzen, D. E. (2003) Folding of DsbB in mixed micelles: a kinetic analysis of the stability of a bacterial membrane protein. *J. Mol. Biol. 330*, 641–649.

28. Miller, D., Charalambous, K., Rotem, D., Schuldiner, S., Curnow, P., and Booth, P. J. (2009) In vitro unfolding and refolding of the small multidrug transporter EmrE. *J. Mol. Biol. 393*, 815–832.

29. Dockter, C., Volkov, A., Bauer, C., Polyhach, Y., Joly-Lopez, Z., Jeschke, G., and Paulsen, H. (2009) Refolding of the integral membrane protein light-harvesting complex II monitored by pulse EPR. *Proc. Natl. Acad. Sci. U.S.A. 106*, 18485–18490.

30. Plumley, F. G., and Schmidt, G. W. (1987) Reconstitution of chlorophyll *a/b* light-harvesting complexes: xanthophyll-dependent assembly and energy transfer. *Proc. Natl. Acad. Sci. U.S.A. 84*, 146–150.

31. McKibbin, C., Farmer, N. A., Edwards, P. C., Villa, C., and Booth, P. J. (2009) Urea unfolding of opsin in phospholipid bicelles. *Photochem. Photobiol. 85*, 494–500.

32. Oprian, D. D., Molday, R. S., Kaufman, R. J., and Khorana, H. G. (1987) Expression of a synthetic bovine rhodopsin gene in monkey kidney cells. *Proc. Natl. Acad. Sci. U.S.A. 84*, 8874–8878.

33. Sreerama, N., and Woody, R. W. (2000) Estimation of protein secondary structure from circular dichroism spectra: comparison of CONTIN, SELCON, and CDSSTR methods with an expanded reference set. *Anal. Biochem. 287*, 252–260.

34. Provencher, S. W., and Glockner, J. (1981) Estimation of globular protein secondary structure from circular dichroism. *Biochemistry 20*, 33–37.

35. Sreerama, N., and Woody, R. W. (1993) A self-consistent method for the analysis of protein secondary structure from circular dichroism. *Anal. Biochem. 209*, 32–44.

36. Manavalan, P., and Johnson, W. C., Jr. (1987) Variable selection method improves the prediction of protein secondary structure from circular dichroism spectra. *Anal. Biochem. 167*, 76–85.

37. Hwang, T. L., and Shaka, A. J. (1995) Water suppression that works. Excitation sculpting using arbitrary wave-forms and pulsed-field gradients. *J. Magn. Reson. A 112*, 275–279.

38. Stott, K., Stonehouse, J., Keeler, J., Hwang, T. L., and Shaka, A. J. (1995) Excitation sculpting in high-resolution nuclear magnetic resonance spectroscopy: application to selective NOE experiments. *J. Am. Chem. Soc. 117*, 4199–4200.

39. Grassetti, D. R., and Murray, J. F., Jr. (1967) Determination of sulfhydryl groups with 2,2'- or 4,4'-dithiodipyridine. *Arch. Biochem. Biophys. 119*, 41–49.

40. Klein-Seetharaman, J., Hwa, J., Cai, K., Altenbach, C., Hubbell, W. L., and Khorana, H. G. (1999) Single-cysteine substitution mutants at amino acid positions 55–75, the sequence connecting the cytoplasmic ends of helices I and II in rhodopsin: reactivity of the sulfhydryl groups and their derivatives identifies a tertiary structure that changes upon light-activation. *Biochemistry 38*, 7938–7944.

41. Farrens, D. L., and Khorana, H. G. (1995) Structure and function in rhodopsin. Measurement of the rate of metarhodopsin II decay by fluorescence spectroscopy. *J. Biol. Chem. 270*, 5073–5076.

42. Chen, Y. S., and Hubbell, W. L. (1978) Reactions of the sulfhydryl groups of membrane-bound bovine rhodopsin. *Membr. Biochem. 1*, 107–130.

43. Sapra, T. K., Park, P. S., Filipek, S., Engel, A., Muller, D. J., and Palczewski, K. (2006) Detecting molecular interactions that stabilize native bovine rhodopsin. *J. Mol. Biol. 358*, 255–269.

44. Rader, A. J., Anderson, G., Isin, B., Khorana, H. G., Bahar, I., and Klein-Seetharaman, J. (2004) Identification of core amino acids stabilizing rhodopsin. *Proc. Natl. Acad. Sci. U.S.A. 101*, 7246–7251.

45. Klein-Seetharaman, J., Getmanova, E. V., Loewen, M. C., Reeves, P. J., and Khorana, H. G. (1999) NMR spectroscopy in studies of light-induced structural changes in mammalian rhodopsin: applicability of solution (19)F NMR. *Proc. Natl. Acad. Sci. U.S.A. 96*, 13744–13749.

46. Kusnetzow, A. K., Altenbach, C., and Hubbell, W. L. (2006) Conformational states and dynamics of rhodopsin in micelles and bilayers. *Biochemistry 45*, 5538–5550.

47. Knudsen, P., and Hubbell, W. L. (1978) Stability of rhodopsin in detergent solutions. *Membr. Biochem. 1*, 297–322.

48. Ramon, E., Marron, J., del Valle, L., Bosch, L., Andres, A., Manyosa, J., and Garriga, P. (2003) Effect of dodecyl maltoside detergent on rhodopsin stability and function. *Vision Res. 43*, 3055–3061.

49. Wallace, B. A., Lees, J. G., Orry, A. J., Lobley, A., and Janes, R. W. (2003) Analyses of circular dichroism spectra of membrane proteins. *Protein Sci. 12*, 875–884.

50. Hirst, J. D., and Brooks, C. L., III (1994) Helicity, circular dichroism and molecular dynamics of proteins. *J. Mol. Biol. 243*, 173–178.

51. Dornmair, K., Kiefer, H., and Jahnig, F. (1990) Refolding of an integral membrane protein. OmpA of *Escherichia coli*. *J. Biol. Chem. 265*, 18907–18911.

52. London, E., and Khorana, H. G. (1982) Denaturation and renaturation of bacteriorhodopsin in detergents and lipid-detergent mixtures. *J. Biol. Chem. 257*, 7003–7011.

53. Ibel, K., May, R. P., Kirschner, K., Szadkowski, H., Mascher, E., and Lundahl, P. (1990) Protein-decorated micelle structure of sodium-dodecyl-sulfate−protein complexes as determined by neutron scattering. *Eur. J. Biochem. 190*, 311–318.

54. Jirgensons, B. (1967) Effects of n-propyl alcohol and detergents on the optical rotatory dispersion of alpha-chymotrypsinogen, beta-casein, histone fraction F1, and soybean trypsin inhibitor. *J. Biol. Chem. 242*, 912–918.

55. Mascher, E., and Lundahl, P. (1989) Sodium dodecyl sulphate-protein complexes: changes in size or shape below the critical micelle concentration, as monitored by high-performance agarose gel chromatography. *J. Chromatogr. A 476*, 147–158.

56. Mattice, W. L., Riser, J. M., and Clark, D. S. (1976) Conformational properties of the complexes formed by proteins and sodium dodecyl sulfate. *Biochemistry 15*, 4264–4272.

57. Rao, J. K., and Argos, P. (1981) Structural stability of halophilic proteins. *Biochemistry 20*, 6536–6543.

58. Tanford, C. (1991) The Hydrophobic Effect. Formation of Micelles and Biological Membranes, 2nd ed., Wiley & Sons, New York.

59. Otzen, D. E. (2002) Protein unfolding in detergents: effect of micelle structure, ionic strength, pH, and temperature. *Biophys. J. 83*, 2219–2230.

60. Otzen, D. E., and Oliveberg, M. (2002) Burst-phase expansion of native protein prior to global unfolding in SDS. *J. Mol. Biol. 315*, 1231–1240.

61. Croonen, Y., Gelade, E., Van der Zegel, M., Van der Auweraer, M., Vandendriessche, H., De Schryver, F. C., and Almgren, M. (1983) Influence of salt, detergent concentration, and temperature on the fluorescence quenching of 1-methylpyrene in sodium dodecyl sulfate with m-dicyanobenzene. *J. Phys. Chem. 87*, 1426–1431.

62. Baldwin, R. L., and Zimm, B. H. (2000) Are denatured proteins ever random coils? *Proc. Natl. Acad. Sci. U.S.A. 97*, 12391–12392.

63. Fedorov, A. N., and Baldwin, T. O. (1995) Contribution of cotranslational folding to the rate of formation of native protein structure. *Proc. Natl. Acad. Sci. U.S.A. 92*, 1227–1231.

64. Makeyev, E. V., Kolb, V. A., and Spirin, A. S. (1996) Enzymatic activity of the ribosome-bound nascent polypeptide. *FEBS Lett. 378*, 166–170.

65. Hessa, T., Kim, H., Bihlmaier, K., Lundin, C., Boekel, J., Andersson, H., Nilsson, I., White, S. H., and von Heijne, G. (2005) Recognition of transmembrane helices by the endoplasmic reticulum translocon. *Nature 433*, 377–381.